Neuron, Vol. 28, 187–196, April, 2000, Copyright ©2000 by Cell Press

The Actions of Synaptically Released Zinc at Hippocampal Mossy Fiber Synapses

Kaspar Vogt,[†‡] Jack Mellor,[†] Gang Tong,[§] and Roger Nicoll*
Department of Cellular and Molecular Pharmacology
Department of Physiology
University of California, San Francisco
San Francisco, California 94143

Summary

Zn^{2+} is present at high concentrations in the synaptic vesicles of hippocampal mossy fibers. We have used Zn^{2+} chelators and the *mocha* mutant mouse to address the physiological role of Zn^{2+} in this pathway. Zn^{2+} is not involved in the unique presynaptic plasticities observed at mossy fiber synapses but is coreleased with glutamate from these synapses, both spontaneously and with electrical stimulation, where it exerts a strong modulatory effect on the NMDA receptors. Zn^{2+} tonically occupies the high-affinity binding site of NMDA receptors at mossy fiber synapses, whereas the lower affinity voltage-dependent Zn^{2+} binding site is occupied during action potential driven–release. We conclude that Zn^{2+} is a modulatory neurotransmitter released from mossy fiber synapses and plays an important role in shaping the NMDA receptor response at these synapses.

Introduction

Ever since the discovery that Zn^{2+} is present in large amounts in discrete areas of the hippocampus (Maske, 1955), there has been intense speculation concerning possible synaptic signaling roles for this metal in brain function. Much has subsequently been learned about the mechanisms involved in the sequestration of Zn^{2+} and its effects in the CNS (Frederickson, 1989). Zn^{2+} is accumulated into synaptic vesicles by a specific Zn^{2+} transporter termed ZnT3 (Palmiter et al., 1996; Wenzel et al., 1997; Cole et al., 1999). Strong electrical stimulation of hippocampal mossy fibers (Assaf and Chung, 1984) or high potassium (Howell et al., 1984; Aniksztejn et al., 1987) elevates the concentration of Zn^{2+} measured in perfusates, suggesting that Zn^{2+} is released from mossy fibers. Despite the enormous amount of work on Zn^{2+} in the CNS suggesting a neurotransmitter role for this metal, an action of synaptically released Zn^{2+} has yet to be identified.

The uniquely high concentrations of Zn^{2+} in the hippocampal mossy fiber pathway (Maske, 1955; McLardy, 1962) has made it the most attractive system for studying possible roles for synaptically released Zn^{2+}. Zn^{2+} has numerous cellular effects, particularly on neurotransmitter receptors (Smart et al., 1994). Perhaps the best characterized interaction is between Zn^{2+} and the NMDA subtype of glutamate receptor (NMDAR) (Peters et al., 1987; Westbrook and Mayer, 1987). Zn^{2+} inhibits NMDARs through two mechanisms (Williams, 1996; Chen et al., 1997; Paoletti et al., 1997; Traynelis et al., 1998; Choi and Lipton, 1999): a high-affinity ($IC_{50} \approx 5$ nM) voltage-independent inhibition, as well as a low-affinity ($IC_{50} \approx 20$ μM at −40 mV) voltage-dependent inhibition of NMDAR function. However, based on NMDAR binding studies (Monaghan and Cotman, 1985) and the observation that synaptic plasticity at the mossy fiber synapse is independent of NMDAR activation (Harris and Cotman, 1986), it was long believed that NMDARs, the most sensitive and well-characterized effectors for Zn^{2+}, were not present at mossy fiber synapses. Thus, the most obvious physiological target for synaptically released Zn^{2+} was lacking. The discovery that mossy fiber synapses do, in fact, possess NMDARs (Weisskopf and Nicoll, 1995) provides a very sensitive means for assaying for the presence of Zn^{2+} in the synaptic cleft of mossy fiber synapses and the likelihood of a physiologically relevant action of Zn^{2+}.

We have, therefore, used the hippocampal mossy fiber pathway as a model system in conjunction with selective Zn^{2+} chelation and the use of a naturally occurring mutant mouse, the *mocha* mutant, which lacks Zn^{2+} in its mossy fiber pathway (Kantheti et al., 1998), to explore possible roles of Zn^{2+} in synaptic transmission. We find that Zn^{2+} does not appear to play a role in activity-dependent forms of plasticity that are specifically expressed at mossy fiber synapses, such as frequency facilitation and NMDAR-independent long-term potentiation (LTP). However, chelating synaptically released Zn^{2+} reveals an inhibition of NMDA receptors at mossy fiber synapses but not at neighboring associational/commissural (A/C) synapses, due to the corelease of Zn^{2+} with glutamate at the mossy fiber. In addition, tetanic stimulation results in a transient inhibition of NMDAR function that is blocked by chelating Zn^{2+}. These results establish that a primary role for Zn^{2+} at mossy fiber synapses is the modulation of NMDARs.

Results

In addition to the uniquely high amounts of Zn^{2+} present in mossy fiber synapses, these synapses also exhibit a number of unusual physiological properties, including robust paired-pulse and frequency facilitation as well as an NMDAR-independent form of LTP (Harris and Cotman, 1986; Regehr et al., 1994; Salin et al., 1996). This association raises the possibility that the presence of Zn^{2+} might be responsible for these physiological properties, and, indeed, it has been reported that Zn^{2+} deprivation in rats actually converts frequency facilitation into a frequency depression (Hesse, 1979). To determine

*To whom correspondence should be addressed (e-mail: nicoll@phy.ucsf.edu).
[†] These authors contributed equally to this work.
[‡] Present address: Harvard Medical School, Department of Neurobiology, 220 Longwood Avenue, Boston, Massachusetts 02115.
[§] Department of Neurology, University of California, San Diego, California 92093.

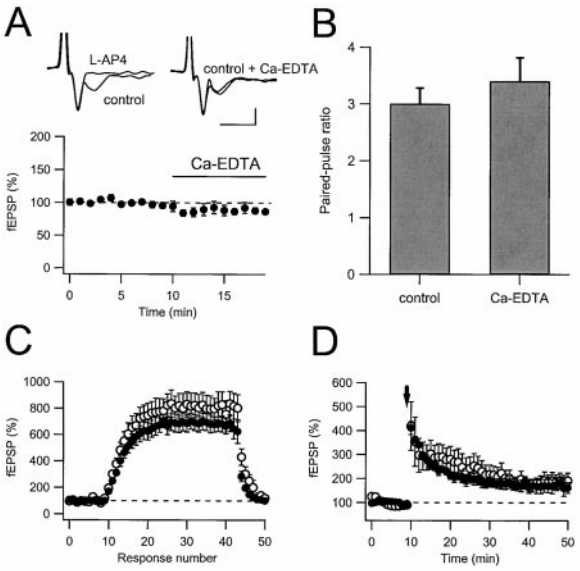

Figure 1. Chelating Extracellular Zn^{2+} Fails to Alter Mossy Fiber Physiology

(A) The Zn^{2+} chelator Ca-EDTA had no effect on mossy fiber fEPSPs. Example fEPSPs generated by a bipolar stimulating electrode placed in the dentate gyrus are shown in control and 5 μM L-AP4 (top left), demonstrating a mossy fiber fEPSP, and in control and 2.5 mM Ca-EDTA (top right). At the bottom is shown an average plot of fEPSP against time with Ca-EDTA bath applied after 10 min (indicated by bar; n = 10).

(B) Paired-pulse ratio is unaffected by the addition of Ca-EDTA. Bar graph demonstrating the average paired-pulse ratios from nine field recordings where two stimuli were given 40 ms apart in the presence and absence of Ca-EDTA.

(C) Frequency facilitation is not affected by the addition of Ca-EDTA. Stimulus frequency was increased from 0.05 Hz to 1 Hz after the tenth stimulus and later returned to 0.05 Hz. The graph shows the averaged results from eight recordings. Closed circles indicate control; open circles indicate the presence of Ca-EDTA.

(D) NMDAR-independent LTP is still present in the presence of Ca-EDTA. A tetanus consisting of 25 Hz for 5 s was given at the time indicated by the arrow; D-APV (100 μM) was present throughout. Closed circles indicate control (n = 3); open circles indicate the presence of Ca-EDTA (n = 6).

whether Zn^{2+} plays a causal role in the specific forms of synaptic plasticity at the mossy fiber system, we examined the effects of applying the extracellular chelator Ca-EDTA (2.5 mM). EDTA binds Zn^{2+} with very high affinity, K_D $10^{-16.4}$, and the apparent affinity constant of Ca-EDTA for Zn^{2+} is in the range of 3–4 nM (Dawson et al., 1986; Bers et al., 1994). Ca-EDTA had no effect at low stimulation frequencies as measured by extracellular field excitatory postsynaptic potential (fEPSP) mediated by AMPA-type glutamate receptors (n = 10) (Figure 1A). The chelator also had no effect on paired-pulse facilitation (control = 3.0 ± 0.3; Ca-EDTA = 3.4 ± 0.4, n = 9, $p > 0.11$) (Figure 1B), frequency facilitation (control = 6.8 ± 0.6; Ca-EDTA = 8.1 ± 1.0, n = 8, $p > 0.09$) (Figure 1C), or the NMDAR-independent type of LTP typical of the mossy fibers (control = 169% ± 30%, n = 3; Ca-EDTA = 184 ± 25%, n = 6, $p > 0.71$) (Figure 1D). These negative results could be due to either the fact that Zn^{2+} is not responsible for these phenomena or the fact that Zn^{2+} acts inside the presynaptic terminal. Additionally, the chelator might have been insufficient at chelating all of the released zinc.

To address these issues, we took advantage of a natural mutant termed the *mocha* mutant, in which the ZnT3 Zn^{2+} transporter is absent from synaptic vesicles and as a consequence the mossy fibers fail to accumulate Zn^{2+}, while leaving other Zn^{2+} stores unchanged (Kantheti et al., 1998). We first confirmed that the mossy fiber pathway in these mice failed to stain for Zn^{2+} (Figure 2A). However, despite the absence of stainable Zn^{2+}, the mossy fiber synapses still showed robust paired-pulse facilitation (Figure $2B_1$). These experiments were repeated in a number of slices from wild-type and *mocha* mice, and no difference was detected in paired-pulse facilitation between the *mocha* (2.15 ± 0.17, n = 5) and wild-type mice (2.46 ± 0.21, n = 4, $p > 0.28$) (Figure $2B_2$). In addition, no difference in frequency facilitation could be seen between the *mocha* (7.17 ± 0.99, n = 5) and wild-type mice (7.75 ± 0.43, n = 4, $p > 0.6$) (Figure 2C). Finally, substantial LTP was recorded in the *mocha* mice (1.84 ± 0.10, n = 5) (Figure 2D). Thus, it appears that the unique physiological properties of the mossy fiber synapses and their uniquely high concentrations of Zn^{2+} are coincidental and unrelated.

As discussed in the Introduction, one of the most sensitive targets for the action of Zn^{2+} is the NMDAR. We, therefore, looked for possible effects of Zn^{2+} on the NMDAR-mediated synaptic responses. Initial experiments were carried out on microdot cultures, where it is possible to control the extracellular environment to a higher degree than is possible in the acute slice preparation. Specifically, an essentially Mg^{2+}-free environment can be obtained and the Zn^{2+} effects on the NMDAR can be studied in isolation. When single neurons are grown in isolation on microdots, they form numerous synapses onto themselves termed autapses (Segal and Furshpan, 1990). Cultures made from the dentate gyrus region contain both granule cells and nongranule cells, which can be distinguished by the selective presynaptic inhibition of the granule cell synaptic responses by the group 3 mGluR agonist, L-AP4 (Tong et al., 1996).

We first examined the effects of Zn^{2+} on the NMDAR-mediated EPSC (NMDAR EPSC) in nongranule cells (i.e., those cells in which L-AP4 had no effect on the synaptic response). Zn^{2+} (10 μM) strongly depressed the NMDAR EPSC, and this depressant effect was largely reversed by the Zn^{2+} chelator BTC-5N (30 μM) (Figure $3A_1$). This effect of BTC-5N was selective in that it had no effect on the depressant action of Mg^{2+} on the NMDAR EPSC (Figure $3A_2$). The results from a number of cells are summarized in Figure 3B and show that the Zn^{2+} inhibition of the NMDAR EPSC (28.8% ± 0.7%, n = 5) is reversed by BTC-5N (84.4% ± 3.0%), while the Mg^{2+} inhibition of the NMDAR EPSC (17.1% ± 1.9%, n = 3) is not reversed by BTC-5N (19.5% ± 1.3%). We next compared the effects of BTC-5N on the NMDAR EPSC recorded in granule cells and nongranule cells. Figure $3C_1$ shows NMDAR EPSCs evoked by two stimuli separated by 50 ms from an isolated neuron. L-AP4 (30 μM) depresses the response, confirming that the cell is a granule cell. Application of BTC-5N enhances the responses. Figure $3C_2$ shows NMDAR EPSCs evoked by three stimuli recorded from a nongranule cell, as defined by the lack

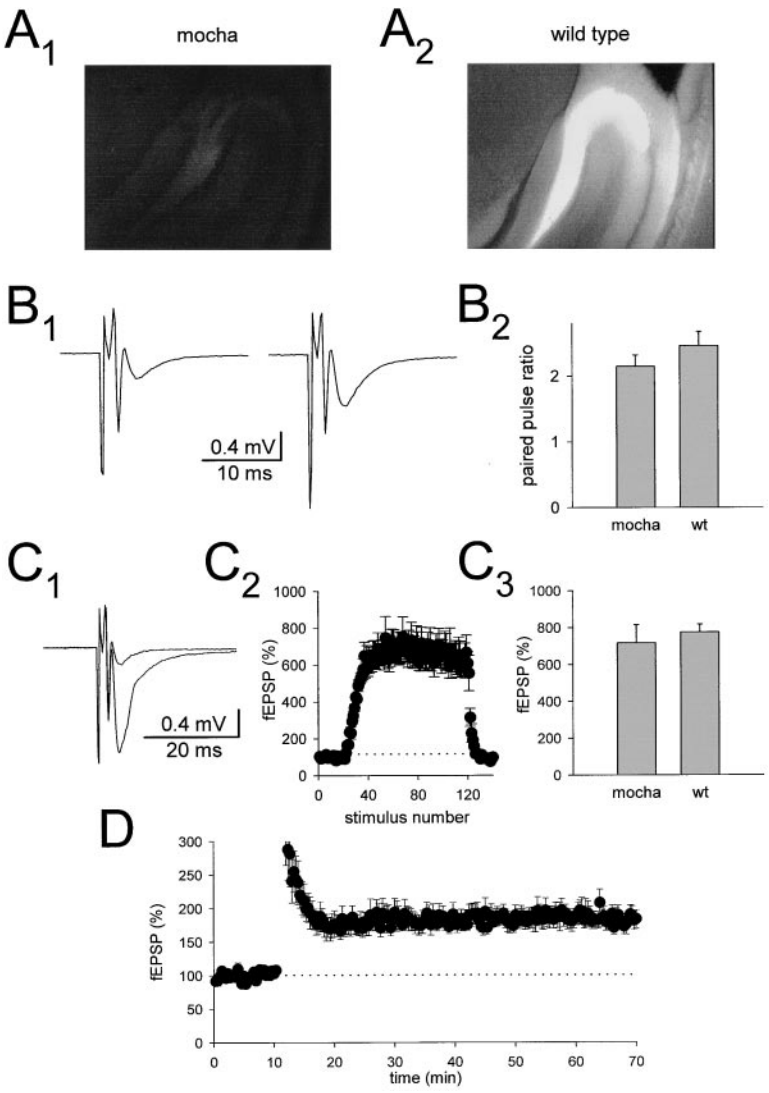

Figure 2. Chelatable Zn^{2+} Is Not Responsible for Characteristic Mossy Fiber Physiology

(A) TSQ stain of a transverse section of mouse hippocampus shows absence of stainable pool of Zn^{2+} in *mocha* mutant mouse (A_1) versus wild-type control (A_2). The two sections were fixated, stained, and imaged on the same coverslip. The bright fluorescent band in the slice of the wild-type animal marks the chelatable pool of Zn^{2+} in the hilus and the s. lucidum of the hippocampus, the mossy fiber area.

(B) Paired-pulse facilitation is characteristically large in mossy fiber fEPSPs recorded from *mocha* mutant mice. Two pulses 40 ms apart were applied to a pair of tungsten stimulus electrodes in the granule cell layer of the dentate gyrus. The resulting fEPSP shows a more than 100% paired-pulse facilitation in the example shown in B_1. The responses from wild-type and *mocha* mice were not significantly different (B_2) in five identical experiments.

(C) Frequency facilitation is not affected in the *mocha* mutant mouse. The stimulus frequency was increased from 0.1 to 1 Hz. Two fEPSPs obtained at the different frequencies are superimposed in an example in C_1. In C_2 the normalized fEPSP amplitude is plotted versus stimulus number for five experiments in *mocha* mutant mice; after 20 pulses the stimulus frequency was increased to 1 Hz during 100 pulses. In C_3 the relative increase in fEPSP amplitude for *mocha* mutant and wild-type mice is shown ($n = 5$).

(D) NMDAR-independent mossy fiber LTP is present in the Zn^{2+}-free *mocha* mouse mutant. The normalized mossy fiber fEPSP amplitude is plotted against time. A 5 s tetanus of 25 Hz was applied to the stimulus electrodes after 10 min ($n = 5$).

of effect of L-AP4. In this case BTC-5N had no effect on the NMDAR EPSC. Results from a number of cells are summarized in Figure 3D and show that in L-AP4-sensitive cells (60.7% $\pm$ 6.8%, $n = 9$) BTC-5N significantly enhanced the NMDAR EPSC (123.9% $\pm$ 3.7%), while in L-AP4-insensitive cells (94.7% $\pm$ 3.2%, $n = 4$) BTC-5N had no effect (102.4% $\pm$ 1.6%). Since the NMDAR EPSC of nongranule cells is sensitive to Zn^{2+} but is unaffected by BTC-5N, and the two types of cells are intermingled on the same culture slips, tonic Zn^{2+} levels in the dish cannot account for the effects of BTC-5N on the granule cell NMDAR EPSC. These results suggest that Zn^{2+} released from the granule cell normally exerts a localized inhibitory effect on the NMDAR EPSC, which can be relieved by a selective Zn^{2+} chelator.

We next returned to the slice preparation to extend these results to a more intact system. We were able to confirm the effects of BTC-5N on mossy fiber NMDAR EPSCs. Cells were held at -40 mV with a reduced Mg^{2+} concentration present in the extracellular solution. The application of BTC-5N (100 μM) reproducibly enhanced the mossy fiber NMDAR EPSC (142% $\pm$ 8%, $n = 7$) (data not shown), suggesting the presence of extracellular Zn^{2+} that inhibits NMDAR function. To characterize further the role of Zn^{2+} at mossy fiber synapses, we used the much higher affinity Zn^{2+} chelator Ca-EDTA which had more dramatic effects compared to BTC-5N. In Figure 4 we compared the effect of Ca-EDTA on the NMDAR EPSC evoked by mossy fiber stimulation and A/C stimulation in the same cells at a negative and positive holding potential. At negative holding potentials the mossy fiber response was considerably and reversibly enhanced (167% $\pm$ 16%, $n = 6$, $p < 0.01$), while the A/C response was unaltered (97% $\pm$ 10%, $n = 6$, $p > 0.76$) (Figure 4A). The rising phase of the mossy fiber NMDAR EPSC varied considerably and was slower than the A/C response. This is presumably related to the asynchrony of the input that can be seen more clearly when the fast rising AMPA EPSC is recorded.

Zn^{2+} is known to block NMDAR function by two mechanisms; a low-affinity, voltage-dependent block and a much higher affinity, voltage-independent block

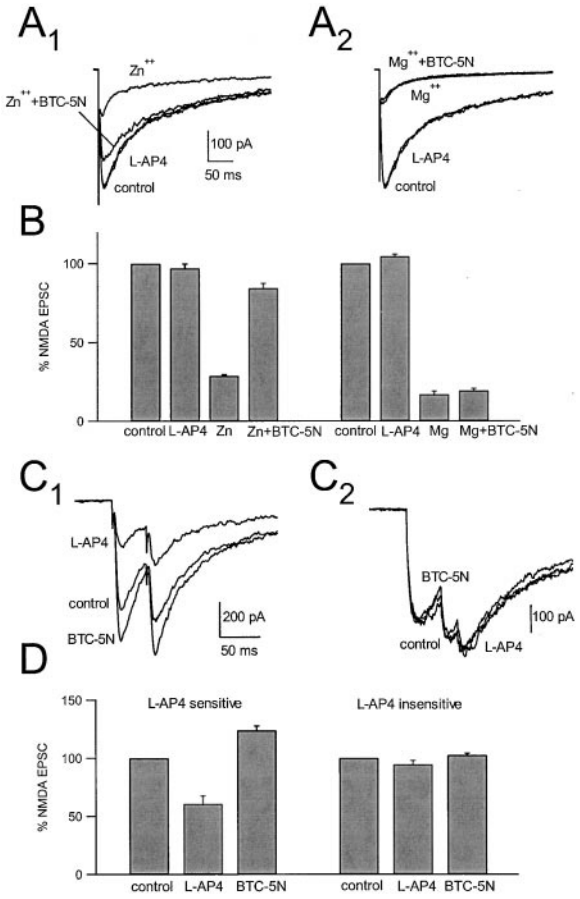

Figure 3. Release of Zn^{2+} from Single Granule Cell Cultures Inhibits Synaptic NMDAR Responses

(A) BTC-5N selectively chelates Zn^{2+}.

(A_1) Averaged autaptic NMDAR EPSCs in control, in the presence of Zn^{2+} (10 μM), or in the presence of Zn^{2+} plus BTC-5N (30 μM) in a L-AP4-insensitive cell (L-AP4, 30 μM).

(A_2) Averaged autaptic NMDAR EPSCs in control, in the presence of Mg^{2+} (50 μM) or in the presence of Mg^{2+} plus BTC-5N (150 μM) in a L-AP4-insensitive cell.

(B) Whereas 30 μM of BTC-5N reversed the Zn^{2+} (10 μM) inhibition (n = 5), 150 μM of BTC-5N had no effect on the Mg^{2+} (50 μM) inhibition of the NMDAR EPSCs (n = 3). L-AP4-insensitive cells were used in this series of experiments, so that the effects of endogenously released Zn^{2+} could be avoided. Holding potential, −70 (A_1) and −80 mV (A_2).

(C) BTC-5N potentiates evoked NMDAR EPSCs in L-AP4-sensitive (C_1) but not in L-AP4-insensitive (C_2) cells. Shown are averaged autaptic NMDAR EPSCs evoked by two (C_1) or three (C_2) stimuli recorded in control, in the presence of BTC-5N (30 μM), and in the presence of L-AP4 (30 μM).

(D) Percent potentiation of the NMDAR EPSC by BTC-5N in L-AP4-sensitive cells (n = 9) and L-AP4-insensitive cells (n = 4). Records are averages of 8–16 sweeps. Holding potential, −70 (C_1) and −80 mV (C_2).

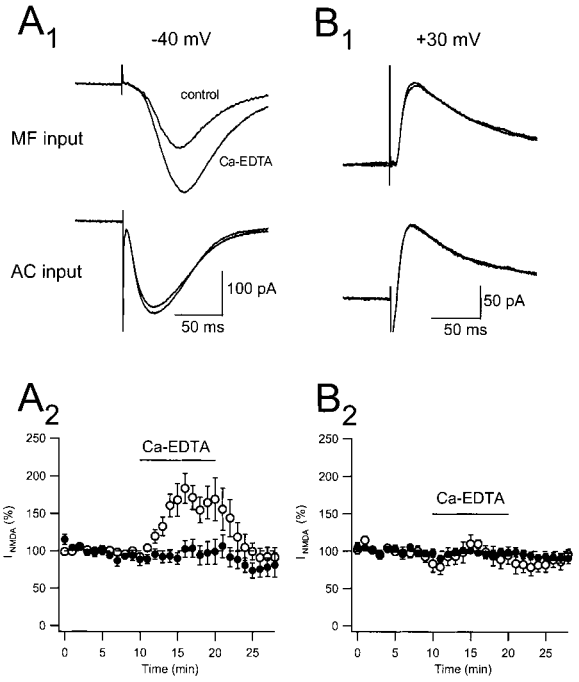

Figure 4. Ca-EDTA Can Remove the Low-Affinity, but Not the High-Affinity, Zn^{2+} Block on Synaptic Mossy Fiber NMDA Responses

(A_1) Example current traces recorded from a cell held at −40 mV in the presence of 0.5 mM Mg^{2+}, 12 μM NBQX, and 100 μM picrotoxin. At the top are responses to stimulation of mossy fibers by a bipolar electrode placed in the dentate gyrus before and after bath application of 2.5 mM Ca-EDTA. At the bottom are the responses to stimulation with a monopolar glass electrode in the stratum radiatum.

(A_2) Graph showing the time course of the increase in mossy fiber but not A/C NMDA response (n = 6). Closed circles are responses to A/C stimulation, open circles to mossy fiber stimulation. Duration of Ca-EDTA addition is represented by the bar.

(B_1) Same as (A_1), but the cell is held at +30 mV in the presence of 1.3 mM Mg^{2+}.

(B_2) Same as (A_2), but for five cells held at +30 mV in 1.3 mM Mg^{2+}.

(Williams, 1996; Chen et al., 1997; Paoletti et al., 1997; Traynelis et al., 1998; Choi and Lipton, 1999). The Zn^{2+} inhibition of NMDAR EPSCs evoked at a negative holding potential could involve both its low- and high-affinity actions, whereas at a positive holding potential the inhibition can only occur via the high-affinity, voltage-independent site. We therefore repeated the Ca-EDTA experiments at a positive holding potential, and in contrast to the results at a negative holding potential the extracellular Zn^{2+} chelator Ca-EDTA had no effect on the mossy fiber NMDAR EPSC (100% ± 10%, n = 5, p > 0.99) (Figure 4B). We note that this dependence on the postsynaptic membrane potential rules out a presynaptic locus for the effect of Ca-EDTA on the NMDAR EPSC. The observation that Zn^{2+} chelation with Ca-EDTA removes only the voltage-dependent inhibition of the NMDAR EPSC is puzzling, as this Zn^{2+} binding site is of lower affinity than the voltage-independent site and, therefore, might be expected to play less of a role in inhibition of NMDARs by Zn^{2+}. BTC-5N (100 μM) also failed to enhance the NMDAR EPSC at positive membrane potentials (n = 4) (data not shown).

We considered three possibile explanations for this result. First, the NMDAR at the mossy fiber synapses may lack the NR2A subunit, which is required for the high-affinity action of Zn^{2+} (Williams, 1996; Paoletti et al., 1997; Choi and Lipton, 1999). This seems unlikely since the NR2A subunit has been shown immunohistochemically to be present in stratum lucidum (Fritschy et al., 1998). In addition, although this is not a strong argument, ifenprodil (1 μM), a drug that selectively

blocks NMDARs which contain the NR2B subunit, causes an identical partial inhibition of the NMDAR EPSC generated by mossy fiber or A/C stimulation ($n = 4$) (data not shown). Second, it is possible that Zn^{2+} is tonically present but Ca-EDTA cannot chelate Zn^{2+} sufficiently at equilibrium to relieve tonic occupancy of the high-affinity Zn^{2+} binding site. We think this is unlikely, as Ca-EDTA has a very high affinity for Zn^{2+} (apparent $K_D = 3$–4 nM), given its stability constant of $10^{-16.4}$ (Dawson et al., 1986; Bers et al., 1994). Finally, the chelator might be present in sufficient quantities to remove ambient Zn^{2+} from all sites, but the Zn^{2+} responsible for the inhibition of the NMDAR EPSC is coreleased with glutamate. The amount of freely available EDTA in our equimolar Ca-EDTA solution is clearly insufficient (Bers et al., 1994) to chelate the concentrations of Zn^{2+} attained in the synaptic cleft after release. The bulk of the released Zn^{2+} therefore has to displace Ca^{2+} from the chelator, a process governed by the unbinding of Ca^{2+} ion and mostly too slow to affect the binding of Zn^{2+} to the high-affinity site (Pearson and DeWit, 1973; Wu et al., 1997).

To distinguish between the last two possibilities, we examined the effect of Ca-EDTA on NMDAR responses evoked by iontophoretically applied glutamate at positive membrane potentials. With this method large NMDA currents can be generated independent of synaptic release. The amount of Zn^{2+} released and the amount of glutamate present at the receptor can therefore be manipulated independently. We first studied the effects of Zn^{2+} chelation in the absence of mossy fiber stimulation. Ca-EDTA (Figure 5) reliably enhanced the NMDAR response evoked by glutamate iontophoresis in s. lucidum but had no effect on the responses generated in s. radiatum. A similar selective enhancement was observed with other Zn^{2+} chelators, including TPEN ($143\% \pm 15\%$, $n = 3$) (data not shown) and dithizone (100 μM) ($193\% \pm 52\%$, $n = 3$) (data not shown), supporting the conclusion that the enhancement is due to the removal of a tonic inhibitory action of endogenous Zn^{2+}. To confirm this conclusion we examined the effect of Ca-EDTA on NMDAR responses evoked by iontophoretically applied glutamate and recorded at positive potentials in the *ZnT3* knockout mouse (Cole et al., 1999). While Ca-EDTA had its usual enhancing action in wild-type mouse ($123\% \pm 3\%$, $n = 3$), no enhancement was observed in the knockout mice ($87\% \pm 3\%$, $n = 4$). It seems, therefore, that there is a significant Zn^{2+}-dependent tonic inhibition of s. lucidum NMDARs, and Ca-EDTA is capable of removing the Zn^{2+} from the high-affinity binding site. This result implies that Zn^{2+} chelation relieves only low-affinity block of the NMDAR EPSC because Ca-EDTA cannot fully chelate the high Zn^{2+} concentration coreleased with glutamate at the mossy fiber synapse.

The experiments thus far indicate that Zn^{2+} is present at mossy fiber synapses and inhibits NMDAR function by acting both at the high- and low-affinity site on the NMDAR and suggest that this Zn^{2+} is synaptically released with stimulation. To more directly address the origin of this extracellular Zn^{2+} and whether its presence is actually dependent on activity, we examined the effect of selectively blocking release from mossy fiber synapses by applying L-AP4 (5 μM) on the NMDAR responses to iontophoretically applied glutamate. L-AP4 reduces both the action potential–dependent release (Lanthorn et al., 1984) as well as the release of miniature synaptic responses (Cotman et al., 1986) from mossy fiber synapses. The size of the iontophoretic NMDAR response evoked in s. lucidum increased in the presence of L-AP4 (Figure 6), consistent with an activity-dependent inhibition of NMDARs. This increase was occluded by the prior application of Ca-EDTA, suggesting that synaptically released Zn^{2+} underlies this effect. In five cells where L-AP4 was applied in the presence and absence of Ca-EDTA, L-AP4 increased the response only in the absence of Ca-EDTA ($203\% \pm 41\%$ versus $72\% \pm 15\%$, $p < 0.05$) (Figure 6D). The responses evoked in s. radiatum were unaffected by L-AP4 or Ca-EDTA ($108\% \pm 6\%$ and $78\% \pm 9\%$, respectively). Tetanic stimulation, which is known to overcome manipulations that inhibit release at mossy fibers (Castillo et al., 1994), resulted in a transient depression of the iontophoretic NMDAR responses to a size similar to that recorded prior to the L-AP4 application (Figures 6A and 6B). This suggests that the release of Zn^{2+} during the tetanus was able to transiently restore the Zn^{2+} inhibition of the NMDARs.

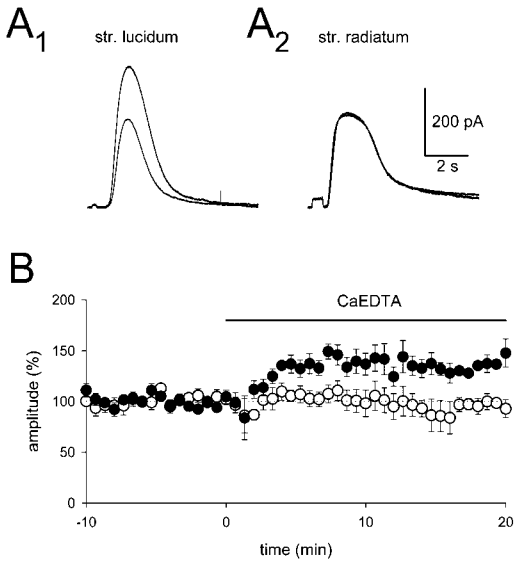

Figure 5. NMDARs in S. Lucidum, but Not in S. Radiatum, Are Tonically Inhibited by Zn^{2+} at Positive Holding Potentials

(A) Sample traces of whole-cell currents from CA3 pyramidal neurons recorded at +30 mV holding potential. CNQX (100 μM) and picrotoxin (100 μM) were present throughout the experiment. NMDAR-mediated whole-cell currents were recorded as a response to iontophoretically applied glutamate to the s. lucidum (A_1) and the s. radiatum (A_2). Iontophoresis electrodes were placed in both the s. lucidum and s. radiatum at the same time so that the size and kinetics of the responses were roughly similar and glutamate applications to each area were interleaved. Application of the high-affinity Zn^{2+} chelator Ca-EDTA (2.5 mM) resulted in a marked increase of the response to s. lucidum iontophoresis (A_1) but no significant change in the response to glutamate application in the s. radiatum (A_2). (B) The average of five experiments with simultaneous s. lucidum (closed circles) and s. radiatum (open circles) application is shown.

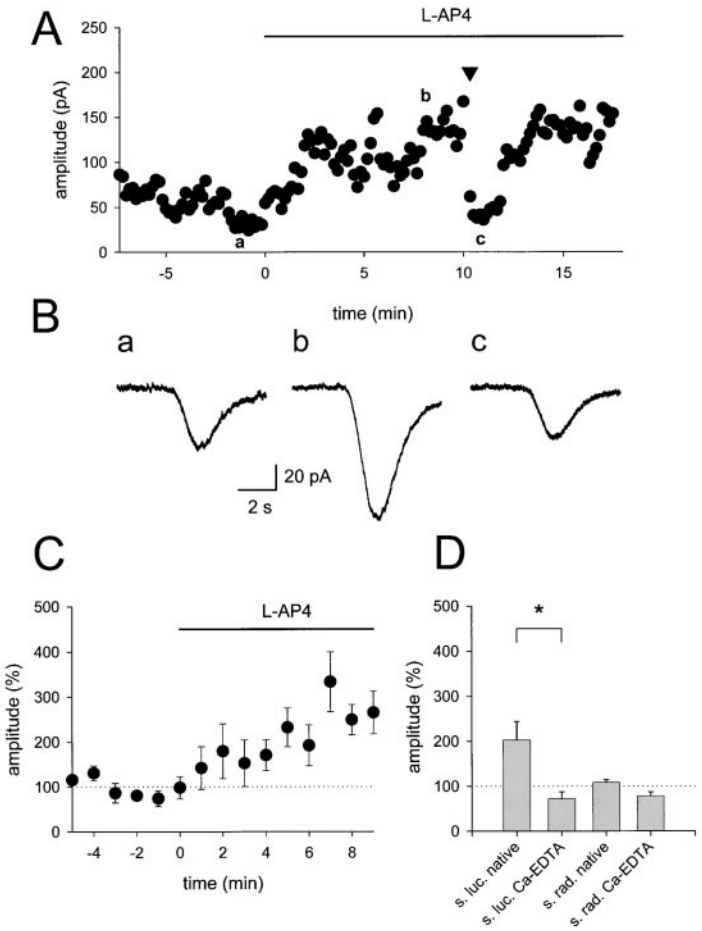

Figure 6. NMDARs in S. Lucidum Show Mossy Fiber Activity-Dependent Inhibition at Negative Holding Potentials

(A) An iontophoresis electrode was placed in s. lucidum, and glutamate was applied to CA3 pyramidal cells held at a holding potential of −40 mV with NBQX (12 μM) and picrotoxin (100 μM) present throughout the experiments. The amplitudes of the resulting NMDAR-mediated whole-cell currents are plotted against time. A bipolar stimulating electrode was inserted in the s. lucidum close to the site of glutamate injection. A 1 s tetanus of 100 Hz was applied at the time marked by the inverted triangle. The group 3 mGluR agonist L-AP4 (10 μM) was applied to the bathing solution at the time indicated.

(B) Sample traces from the same experiment at the times indicated by the letters. L-AP4 application caused a significant increase in the NMDAR response that could be reversed by maximal stimulation of the mossy fiber bundle.

(C) The amplitude of the NMDAR-mediated whole-cell currents was normalized, and the average of four experiments is plotted against time. L-AP4 was included at the time marked zero.

(D) In five cells the effect of L-AP4 on iontophoretic NMDAR responses was compared in the presence and absence of Ca-EDTA.

To confirm that this transient inhibition is, in fact, due to the release of Zn^{2+} during the tetanus, we examined the ability of Ca-EDTA to block the inhibition. This experiment was carried out entirely in the presence of L-AP4 to avoid interference from spontaneously released Zn^{2+}. Once the tetanus-induced inhibition was observed (Figure 7A), Ca-EDTA was applied, which essentially abolished the inhibition (Figure 7B). This blocking action of Ca-EDTA on the tetanus-induced inhibition was reversible (Figure 7C). A summary of the results from all the cells is shown in Figure 7D.

Discussion

Although a great deal of work has been done on characterizing a variety of aspects of Zn^{2+} in the CNS, a function for synaptically released Zn^{2+} has not been described. Because of the extremely high levels of Zn^{2+} in the hippocampal mossy fiber system, we have used this system as a model to address this issue. We first examined the possibility that Zn^{2+} might be responsible for the unusual physiological properties of the mossy fiber synapse, including robust paired-pulse and frequency facilitation and NMDAR-independent LTP, as it has been reported that frequency facilitation is absent in Zn^{2+}-deficient rats (Hesse, 1979). We have found that mossy fiber short-term or long-term plasticity appear unaltered when extracellular Zn^{2+} is chelated with Ca-EDTA. In addition, we have found no alterations in these physiological processes in the *mocha* mutant, a mouse that lacks chelatable Zn^{2+} in the mossy fiber pathway (Kantheti et al., 1998). Finally, in the *ZnT3* knockout mouse (Cole et al., 1999) no clear physiological deficits have been detected in responses to mossy fiber stimulation (P. Schwartzkroin, R. Palmiter, and colleagues, personal communication). We are, thus, unable to explain the difference between these and previous results (Hesse, 1979), although the effect might be due to a secondary effect of chronic Zn^{2+} deficiency.

One of the most thoroughly characterized actions of Zn^{2+} is its inhibition of NMDAR function (Peters et al., 1987; Westbrook and Mayer, 1987). Zn^{2+} appears to act on NMDARs at two distinct sites, resulting in a low-affinity, voltage-dependent inhibition and a high-affinity, voltage-independent inhibition (Williams, 1996; Chen et al., 1997; Paoletti et al., 1997; Traynelis et al., 1998; Choi and Lipton, 1999). Saturation of the high-affinity site results in a substantial (40% according to Williams, 1996, and Chen et al., 1997; 75% according to Paoletti et al., 1997) but incomplete block of the channel. Although it has long been believed that NMDARs are absent at mossy fiber synapses, the demonstration of their activation at these synapses (Weisskopf and Nicoll, 1995) provides a very sensitive target for synaptically released Zn^{2+} at mossy fibers.

Studies in a simplified single-cell culture preparation

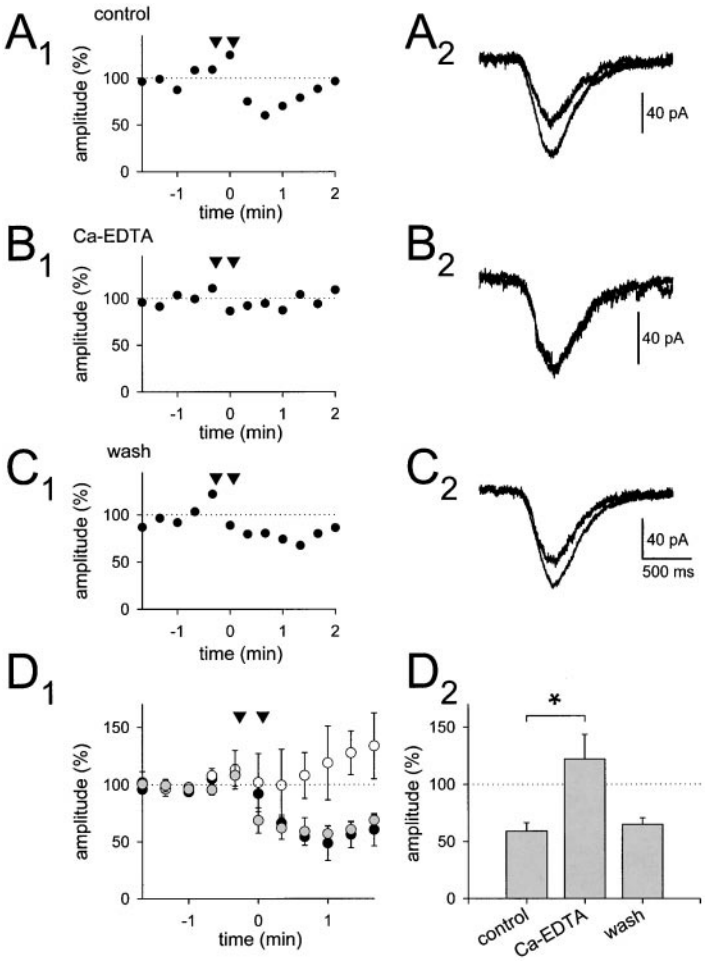

Figure 7. Activity-Dependent Zinc Release by Mossy Fibers Is Responsible for the Inhibition of S. Lucidum NMDARs

The experimental setup is the same as in Figure 6. L-AP4 (10 μM) is present throughout the experiment. (A) through (C) show the responses from one sample experiment. Two 1 s tetani of 100 Hz were applied to the bipolar tungsten electrodes in the s. lucidum, indicated by the arrows.

(A) Baseline response.

(A_1) The normalized amplitude of the NMDAR-mediated whole-cell current is plotted against time.

(A_2) Sample traces of the responses before and after the application of the tetani to s. lucidum.

(B) Ca-EDTA (2.5 mM) was applied to the superfusion solution, and the strength of the iontophoresis electrode was adjusted so that the whole-cell response remained roughly constant. The same tetani were applied again.

(C) The procedure was repeated a third time after the washout of Ca-EDTA.

(D_1) The average of four identical experiments is shown. The average amplitudes are shown superimposed for baseline responses to tetani (black), during the application of Ca-EDTA (white), and after the washout of the Zn^{2+} chelator (gray).

(D_2) The relative change in NMDAR-mediated current due to s. lucidum tetani for the same experiments with the four responses before and after both tetani averaged together. The Zn^{2+} chelator Ca-EDTA blocks the activity-dependent inhibition of s. lucidum NMDARs.

provided the first evidence that Zn^{2+} released from granule cell synapses has functional consequences. Thus, the Zn^{2+} chelator BTC-5N enhanced NMDAR EPSCs evoked in granule cells, but not in nongranule cells in the same cultures. Because of the relatively low affinity of BTC-5N for Zn^{2+} (~0.2 μM) (Haugland, 1996), this enhancement most likely reflects an inhibitory effect of endogenous Zn^{2+} on the low-affinity binding site. Experiments in the slice preparation support this conclusion. BTC-5N was found to enhance the NMDAR EPSC evoked by mossy fiber stimulation at negative potentials but not at positive potentials. Thus, the findings in culture suggest that release of Zn^{2+} from granule cells inhibits its NMDAR function, at least at the low-affinity binding site.

The action of endogenous Zn^{2+} on NMDARs was examined in more detail in the slice preparation with the higher affinity Zn^{2+} chelator Ca-EDTA. The enhancement of mossy fiber NMDAR EPSCs by Ca-EDTA was significantly larger than for BTC-5N, and the simultaneously recorded A/C NMDAR EPSC was unaffected. When these experiments were repeated at a positive holding potential, Ca-EDTA had no effect on either of the synaptic responses. However, Ca-EDTA is capable of relieving the high-affinity block under near equilibrium conditions with iontophoretically evoked NMDAR currents. Two lines of evidence indicate that this enhancing action of Ca-EDTA was due to the chelation of Zn^{2+}. First, the effect could be mimicked with other Zn^{2+} chelators (TPEN and dithizone), and second, we were unable to observe the enhancing action of Ca-EDTA in the *ZnT3* knockout mouse (Cole et al., 1999). The lack of effect of Ca-EDTA on the mossy fiber NMDAR EPSC recorded at positive potentials suggests that Zn^{2+} is coreleased at the synapses with glutamate, and that Ca-EDTA cannot adequately chelate this large and rapid transient of Zn^{2+}. One caveat that should be kept in mind is that extrasynaptic NMDARs may contribute to the iontophoretic responses, and it is a formal possibility that their sensitivity to Zn^{2+} is higher than that of the synaptic receptors.

The present results allow us to provide a rough estimate of the concentration of Zn^{2+} in the extracellular space. The finding that the low-affinity site is bound by Zn^{2+} indicates that Zn^{2+} must reach a concentration in excess of 10–20 μM at mossy fiber synapses. The failure of Ca-EDTA to enhance NMDAR responses in the s. radiatum argues that the extracellular concentration of Zn^{2+} in this region is below nanomolar concentrations, although, as discussed in the Results, this assumes that the receptors in s. radiatum and s. lucidum have the same sensitivity to Zn^{2+}. If s. radiatum NMDARs were to lack the high-affinity site, this estimate would increase to below micromolar concentrations. Given the high concentration of Zn^{2+} in s. lucidum, this would require

a very effective removal mechanism to maintain Zn^{2+} at such low levels in the s. radiatum region.

Direct evidence for synaptic release of Zn^{2+} from mossy fiber terminals comes from the observation that tetanic stimulation of mossy fibers causes a transient depression in NMDAR responses, and this depression is prevented by Ca-EDTA. This observation shows convincingly that Zn^{2+} can be released from mossy fiber synapses during repetitive electrical stimulation. An interesting question that cannot be definitively answered with the present experiments is the kinetics of action of synaptically released Zn^{2+}. Our data is most consistent with a peak concentration of more than 100 μM. The clearance of Zn^{2+} from the synaptic cleft is likely to be relatively slow, compared to glutamate (Tong et al., 1996), due to binding to fixed buffers, such as the NMDAR. In outside-out CA3 dendritic patches (Spruston et al., 1995), 1 ms coapplications of Zn^{2+} with glutamate causes, via the low-affinity binding site, a ~10%–20% decrease in the peak of the NMDAR response. If the clearance of Zn^{2+} from the synaptic cleft were slower than from the outside-out patches, the inhibitory effect would be substantially greater, since Zn^{2+} is an open channel blocker at the low-affinity site. Following a tetanus to the mossy fibers, the NMDA response required more than a minute to recover, suggesting that the clearance of Zn^{2+} following a tetanus is relatively slow. The kinetics of the blocking action of Zn^{2+} at the high-affinity site has not been addressed in this study, and it may well be fully occupied at basal conditions at the mossy fiber synapses, thus reducing the NMDAR response considerably. This could account, at least in part, for the substantially higher AMPAR/NMDAR ratio for the mossy fiber EPSCs compared to the A/C EPSCs (Weisskopf and Nicoll, 1995).

In summary, the present results establish that the metal ion Zn^{2+} is a neurotransmitter and that the activity-dependent synaptic release of Zn^{2+} modulates NMDAR function. This modulation involves an inhibition mediated by both the high-affinity, voltage-independent binding site and the low-affinity, voltage-dependent binding site of Zn^{2+} on the NMDAR. The action of Zn^{2+} appears to be quite local in that we could find no evidence for the presence of extracellular Zn^{2+} in the neighboring s. radiatum.

One of the hallmarks of the mossy fiber synapse is its apparent lack of NMDAR-dependent synaptic plasticity. An intriguing explanation for this unusual feature is that Zn^{2+} prevents adequate activation of the NMDARs. An interesting possibility is that a window might exist between initial synapse formation and the large accumulation of Zn^{2+} in the mossy fiber synapses (Zimmer and Haug, 1978; Frederickson et al., 1981; Gaarskjaer, 1986). If such a window exists, NMDAR-dependent plasticity could play a critical role during synapse formation, as has recently been demonstrated at mossy fiber synapses (Kavalali et al., 1999), but once formed the accumulation of Zn^{2+} would prevent further modification. This is in keeping with the concept of the mossy fiber system acting as a detonator or teacher (Treves and Rolls, 1992) in an associative network, in which case associative plasticity at this synapse in the adult would serve little purpose.

It has recently been reported (Zheng et al., 1998; but see Xiong et al., 1999) that the binding of Zn^{2+} to expressed NMDA receptors at the high-affinity site is reduced by NR2A subunit receptor phosphorylation through the tyrosine kinase Src. Such a mechanism in pyramidal cells in the CA3 area could dynamically adjust the NDMAR EPSC size at the mossy fiber synapses.

The modulation of NMDA receptors might not be the only consequence of synaptically released Zn^{2+}. Several reports have found that Zn^{2+} can enter the postsynaptic cell via a number of routes, including NMDA receptors (Koh and Choi, 1994), Ca^{2+}-permeable AMPA/kainate receptors (Yin and Weiss, 1995), and voltage-gated calcium channels (Weiss et al., 1993; Atar et al., 1995). Zn^{2+} is known to activate a number of transcription factors such as Egr1 (Park and Koh, 1999) and NF κB (Shumilla et al., 1998) and to affect other second messenger systems such as PKC (Hubbard et al., 1991) and calmodulin (Brewer et al., 1979). An intriguing possibility is that mossy fiber synapses, as a consequence of Zn^{2+} entry into the postsynaptic cell via the NMDARs localized at the mossy fiber synapses, could modify intracellular signaling pathways or, given their close proximity to the cell body, directly control gene transcription.

Experimental Procedures

Transverse sections of guinea pig and mouse hippocampi were obtained using standard methods. For guinea pigs hippocampi were dissected out of the brain and 300–500 μm thick slices were obtained using a vibrating microtome (Leica, Germany). For mice each hemisphere was cut into saggital slices of 300–500 μm in thickness. Slices were placed in artificial cerebrospinal fluid (ACSF) at room temperature for at least 1 hr prior to performing experiments. The slices were then transferred to a holding chamber mounted on an upright microscope (Olympus BX50WI, USA), where they were continuously superfused with ACSF equilibrated with 95% O_2 and 5% CO_2 at room temperature. Unless otherwise noted, ACSF contained (in mM): NaCl 119, $NaHCO_3$ 26, glucose 11, KCl 2.5, $CaCl_2$ 2.5, $MgSO_4$ 1.3, and NaH_2PO_4 1. For whole-cell recordings cells were visualized using Nomarski-type differential interference contrast imaging with infrared illumination. Images were captured with a CCD camera (Hamamatsu, Japan) and displayed on a video screen. Whole-cell currents from CA3 pyramidal cells were measured with the patch-clamp technique in the whole-cell configuration. The pipette solution (pH 7.4, 280 mOsm) contained (in mM): K gluconate 110, QX-314Cl 5, NaCl 8, HEPES 10, EGTA 0.2, MgATP 4, and Na_3GTP 0.3, for experiments done at negative holding potentials. Experiments at +30 mV were done using a solution containing (in mM): Cs gluconate 107, TEACl 10, QX-314Cl 5, NaCl 8, HEPES 10, EGTA 0.2, MgATP 4, and Na_3GTP 0.3. Borosilicate glass pipettes were pulled to tip resistances between 2–4 MΩ on a horizontal electrode puller (Sutter, Novato USA). Access resistances were between 10 and 20 MΩ and were continuously monitored.

fEPSPs were recorded with extracellular electrodes filled with ACSF (2–4 MΩ). Bipolar tungsten electrodes were placed in the granule cell layer of the dentate gyrus in order to elicit mossy fiber responses. In mice the group 2 metabotropic glutamate receptor agonist DCGIV was used at the end of the experiments to verify that the signal was generated by mossy fiber inputs. In guinea pigs the group 3 metabotropic glutamate receptor agonist L-AP4 was used to identify mossy fiber inputs. To induce zinc release from mossy fiber terminals during iontophoresis, the stimulus electrodes were placed in s. lucidum close to the site of iontophoresis to ensure overlapping fields of influence.

Iontophoresis electrodes were pulled from borosilicate glass and filled with 1M Na glutamate at a pH of 8–9. Electrode resistances were between 70 and 100 MΩ. Glutamate was ejected using a constant current iontophoresis instrument (WPI, USA) with pulses up to 1 μA for 5–50 ms. Electrodes were lowered onto the surface of

the preparation under visual control. For dual application one of the electrodes was placed onto the s. lucidum near the stem dendrite of the patched pyramidal cell; the other electrode was placed on the surface of s. radiatum. The iontophoretic strengths and the positions of the electrodes were adjusted until the size and rise time of the evoked currents were comparable at both sites. Due to the high resistance of the iontophoresis electrodes, a leak of glutamate was rarely observed; in those cases a backing current of 2–10 nA was applied and its magnitude adjusted until it disappeared. Data were collected using Neurophysiologia software (D. Selig) or Igor Pro (Wavemetrics) and analyzed online. Synaptic responses were filtered at 2–5 kHz and digitized at 5 kHz; iontophoretic signals were filtered at 500 Hz and digitized at 1 kHz. Iontophoretic pulses were applied every 20–60 s, synaptic responses were evoked every 15–30 s. For dual pathway experiments, the inputs were stimulated alternately.

Autapse cultures were prepared as previously discribed (Tong et al., 1996). In brief, microdot cultures were prepared from hippocampal neurons of the dentate region from prenatal day 35–55 guinea pig fetuses. Whole-cell recordings were made with patch pipettes containing (in mM): K-gluconate 110, NaCl 10, HEPES 10, EGTA 10, MgATP 4, GTP 0.2, and K_2-creatine phosphate 20 as well as 50 U/ml phosphocreatine kinase (adjusted to pH 7.3 with KOH). The extracellular medium, which was made with HPLC grade water and ultra pure reagents, contained (in mM): NaCl 140 mM, KCl 3.5 mM, HEPES 10 mM, glucose 20 mM, $CaCl_2$ 2 mM, 50 μM picrotoxin, 10 μM CNQX, and 20 μM glycine (adjusted to pH 7.4 with NaOH).

To stain slices for Zn^{2+}, the slices were dehydrated in ice-cold methanol for 5 min and fixated in ice-cold acetone for another 5 min. They were then washed twice in PBS for 5 min and placed on a glass specimen holder. The TSQ dye was prepared as follows: 5 mg TSQ was dissolved in 333 μl ethanol by gentle heating in a water bath and frequent vortexing; 10 μl of this solution was added to 5 ml H_2O in which 95 mg Na acetate and 145 mg Na barbital had been dissolved. The solutions were prepared fresh for every staining. Slices from *mocha* mice and wild-type controls were fixated at the same time and mounted, stained, and visualized side by side. TSQ and BTC-5N were obtained from Molecular Probes, and all other chemicals were obtained from Tocris and Sigma USA. Ca-EDTA was prepared as a 1:1 mixture and the pH adjusted to 7.3 with NaOH. All measurements are given as mean ± SEM. Statistical significance was tested using the Student's t test.

Acknowledgments

We thank Dr. R. Palmiter and T. Cole (University of Washington) for the *ZnT3* knockout mice and Drs. P. Schwartzkroin and V. Lopantsev (University of Washington) for sharing unpublished results. We are grateful for valuable input on zinc staining from Drs. J. Gitschier and Y.-M. Kuo (University of California, San Francisco,) and for generous assistance with the *mocha* mutant mice by Dr. R. B. Kelly (University of California, San Francisco). We thank Drs. M. Frerking and M. Scanziani for their comments on the manuscript and H. Czerwonka for help in preparing the manuscript. K. E. V. was supported by a grant from the Swiss National Science Foundation, J. M. by a Wellcome Trust Travelling Fellowship, and G. T. by a National Institute of Mental Health postdoctoral fellowship. R. A. N. is a member of the Keck Center for Integrative Neuroscience and the Silvio Conte Center for Neuroscience Research. He is supported by grants from the National Institutes of Health and the Bristol-Myers Squibb Corporation.

Received November 11, 1999; revised February 7, 2000.

References

Aniksztejn, L., Charton, G., and Ben-Ari, Y. (1987). Selective release of endogenous zinc from the hippocampal mossy fibers in situ. Brain Res. *404*, 58–64.

Assaf, S.Y., and Chung, S.-H. (1984). Release of endogenous Zn^{2+} from brain tissue during activity. Nature *308*, 734–736.

Atar, D., Backx, P.H., Appel, M.M., Gao, W.D., and Marban, E. (1995). Excitation-transcription coupling mediated by zinc influx through voltage-dependent calcium channels. J. Biol. Chem. *270*, 2473–2477.

Bers, D.M., Patton, C., and Nuccitelli, R. (1994). A practical guide to the preparation of Ca buffers. Methods Cell Biol. *40*, 3–29.

Brewer, G.J., Aster, J.C., Knutsen, C.A., and Kruckeberg, W.C. (1979). Zinc inhibition of calmodulin: a proposed molecular mechanism of zinc action on cellular functions. Am. J. Hematol. *7*, 53–60.

Castillo, P.E., Weisskopf, M.G., and Nicoll, R.A. (1994). The role of Ca^{2+} channels in hippocampal mossy fiber synaptic transmission and long-term potentiation. Neuron *12*, 261–269.

Chen, N., Moshaver, A., and Raymond, L.A. (1997). Differential sensitivity of recombinant N-methyl-D-aspartate receptor subtypes to zinc inhibition. Mol. Pharmacol. *51*, 1015–1023.

Choi, Y.B., and Lipton, S.A. (1999). Identification and mechanism of action of two histidine residues underlying high-affinity Zn^{2+} inhibition of the NMDA receptor. Neuron *23*, 171–180.

Cole, T.B., Wenzel, H.J., Kafer, K.E., Schwartzkroin, P.A., and Palmiter, R.D. (1999). Elimination of zinc from synaptic vesicles in the intact mouse brain by disruption of the ZnT3 gene. Proc. Natl. Acad. Sci. USA *96*, 1716–1721.

Cotman, C.W., Flatman, J.A., Ganong, A.H., and Perkins, M.N. (1986). Effects of excitatory amino acid antagonists on evoked and spontaneous excitatory potentials in guinea pig hippocampus. J. Physiol. *378*, 403–415.

Dawson, R.M.C., Elliot, D.C., Elliot, W.H., and Jones, K.M. (1986). Data for Biochemical Research, Third Edition (New York: Oxford Science).

Frederickson, C.J. (1989). Neurobiology of zinc and zinc-containing neurons. Int. Rev. Neurobiol. *31*, 145–238.

Frederickson, C.J., Howell, G.A., and Frederickson, M.H. (1981). Zinc dithizonate staining in the cat hippocampus: relationship to mossy-fiber neuropil and postnatal development. Exp. Neurol. *73,* 812–823.

Fritschy, J.M., Weinmann, O., Wenzel, A., and Benke, D. (1998). Synapse-specific localization of NMDA and GABA(A) receptor subunits revealed by antigen-retrieval immunohistochemistry. J. Comp. Neurol. *390*, 194–210.

Gaarskjaer, F.B. (1986). The organization and development of the hippocampal mossy fiber system. Brain Res. *396*, 335–357.

Harris, E.W., and Cotman, C.W. (1986). Long-term potentiation of guinea-pig mossy fiber responses is not blocked by N-methyl-D-aspartate antagonists. Neurosci. Lett. *70*, 132–137.

Haugland, H.P. (1996). Handbook of Fluorescent Probes and Research Chemicals, Sixth Edition (Eugene, Oregon: Molecular Probes).

Hesse, G.W. (1979). Chronic zinc deficiency alters neuronal function of hippocampal mossy fibers. Science *205*, 1005–1007.

Howell, G.A., Welch, M.G., and Frederickson, C.J. (1984). Stimulation-induced uptake and release of zinc in hippocampal slices. Nature *308*, 736–738.

Hubbard, S.R., Bishop, W.R., Kirschmeier, P., George, S.J., Cramer, S.P., and Hendrickson, W.A. (1991). Identification and characterization of zinc binding site in protein kinase C. Science *254*, 1776–1779.

Kantheti, P., Qiao, X., Diaz, M.E., Peden, A.A., Meyer, G.E., Carskadon, S.L., Kapfhamer, D., Sufalko, D., Robinson, M.S., Noebels, J.L., and Burmeister, M. (1998). Mutation in AP-3 delta in the mocha mouse links endosomal transport to storage deficiency in platelets, melanosomes, and synaptic vesicles. Neuron *21*, 111–122.

Koh, J.Y., and Choi, D.W. (1994). Zinc toxicity on cultured cortical neurons: involvement of N-methyl-D-aspartate receptors. Neuroscience *60*, 1049–1057.

Kavalali, E.T., Klingauf, J., and Tsien, R.W. (1999). Activity-dependent regulation of synaptic clustering in a hippocampal culture system. Proc. Natl. Acad. Sci. USA *96*, 12893–12900.

Lanthorn, T.H., Ganong, A.H., and Cotman, C.W. (1984). 2-amino-4-phosphonobutyrate selectively blocks mossy fiber-CA3 responses in guinea pig but not rat hippocampus. Brain Res. *290*, 174–178.

Maske, H. (1955). Uber den topochemischen nachwels von zink

im ammonshorn verschiedener saugetiere. Naturwissenschaften *42*, 424.

McLardy, T. (1962). Zinc enzymes and the hippocampal mossy fibre system. Nature *194*, 300–302.

Monaghan, D.T., and Cotman, C.W. (1985). Distribution of N-methyl-D-aspartate-sensitive L-[^{3}H]glutamate-binding sites in rat brain. J. Neurosci. *5*, 2909–2919.

Palmiter, R.D., Cole, T.B., Quaife, C.J., and Findley, S.D. (1996). ZnT-3, a putative transporter of zinc into synaptic vesicles. Proc. Natl. Acad. Sci. USA *93*, 14934–14939.

Paoletti, P., Ascher, P., and Neyton, J. (1997). High-affinity zinc inhibition of NMDA NR1–NR2A receptors. J. Neurosci. *17*, 5711–5725. Erratum: J. Neurosci. *17*(20), 1997.

Park, J.A. and Koh, J.Y. (1999). Induction of an immediate early gene egr-1 by zinc through extracellular signal-regulated kinase activation in cortical culture: its role in zinc-induced neuronal death. J. Neurochem. *73*, 450–456.

Pearson, R.G. and DeWit, D.G. (1973). Kinetic behavior of aminopolycarboxylate ligands in substitution reactions on Zn(II) complexes. Coord. Chem. *2*, 175–184.

Peters, S., Koh, J., and Choi, D.W. (1987). Zinc selectively blocks the action of N-methyl-D-aspartate on cortical neurons. Science *236*, 589–593.

Regehr, W.G., Delaney, K.R., and Tank, D.W. (1994). The role of presynaptic calcium in short-term enhancement at the hippocampal mossy fiber synapse. J. Neurosci. *14*, 523–537.

Salin, P.A., Scanziani, M., Malenka, R.C., and Nicoll, R.A. (1996). Distinct short-term plasticity at two excitatory synapses in the hippocampus. Proc. Natl. Acad. Sci. USA *93*, 13304–13309.

Segal, M.M., and Furshpan, E.J. (1990). Epileptiform activity in microcultures containing small numbers of hippocampal neurons. J. Neurophysiol. *64*, 1390–1399.

Shumilla, J.A., Wetterhahn, K.E., and Barchowsky, A. (1998). Inhibition of NF-kappa B binding to DNA by chromium, cadmium, mercury, zinc, and arsenite in vitro: evidence of a thiol mechanism. Arch. Biochem. Biophys. *349*, 356–362.

Smart, T.G., Xie, X., and Krishek, B.J. (1994). Modulation of inhibitory and excitatory amino acid receptor ion channels by zinc. Prog. Neurobiol. *42*, 393–441.

Spruston, N., Jonas, P., and Sakmann, B. (1995). Dendritic glutamate receptor channels in rat hippocampal CA3 and CA1 pyramidal neurons. J. Physiol. (Lond.) *482*, 325–352.

Tong, G., Malenka, R.C., and Nicoll, R.A. (1996). Long-term potentiation in cultures of single hippocampal granule cells: a presynaptic form of plasticity. Neuron *16*, 1147–1157.

Traynelis, S.F., Burgess, M.F., Zheng, F., Lyuboslavsky, P., and Powers, J.L. (1998). Control of voltage-independent zinc inhibition of NMDA receptors by the NR1 subunit. J. Neurosci. *18*, 6163–6175.

Treves, A., and Rolls, E.T. (1992). Computational constraints suggest the need for two distinct input systems to the hippocampal CA3 network. Hippocampus *2*, 189–199.

Weiss, J.H., Hartley, D.M., Koh, J.Y., and Choi, D.W. (1993). AMPA receptor activation potentiates zinc neurotoxicity. Neuron *10*, 43–49.

Weisskopf, M.G., and Nicoll, R.A. (1995). Presynaptic changes during mossy fiber LTP revealed by NMDA receptor-mediated synaptic responses. Nature *376*, 256–259.

Wenzel, H.J., Cole, T.B., Born, D.E., Schwartzkroin, P.A., and Palmiter, R.D. (1997). Ultrastructural localization of zinc transporter-3 (ZnT-3) to synaptic vesicle membranes within mossy fiber boutons in the hippocampus of mouse and monkey. Proc. Natl. Acad. Sci. USA *94*, 12676–12681.

Westbrook, G.L., and Mayer, M.L. (1987). Micromolar concentrations of Zn^{2+} antagonize NMDA and GABA responses of hippocampal neurons. Nature *328*, 640–643.

Williams, K. (1996). Separating dual effects of zinc at recombinant N-methyl-D-asparate receptors. Neurosci. Lett. *215,* 9–12.

Wu, S.L., Johnson, K.A., and DeW Horrocks, W., Jr. (1997). Kinetics of formation of Ca^{2+} complexes of acyclic and macrocyclic poly (aminocarboxylate) ligands: bimolecular rate constants for the fully-deprotonated ligands reveal the effect of macrocyclic ligand constraints on the rate-determining conversions of rapidly-formed intermediates to the final complexes. Inorg. Chem. *36*, 1884–1889.

Xiong, Z.-G., Pelkey, K.A., Lu, W.Y., Lu, Y.M., Roder, J.C., MacDonald, J.F., and Salter, M.W. (1999). Src potentiation of NMDA receptors in hippocampal and spinal neurons is not mediated by reducing zinc inhibition. J. Neurosci. *19*, 5889–5997.

Yin, H.Z., and Weiss, J.H. (1995). Zn(2+) permeates Ca(2+) permeable AMPA/kainate channels and triggers selective neural injury. Neuroreport *6*, 2553–2556.

Zheng, F., Gingrich, M.B., Traynelis, S.F., and Conn, P.J. (1998). Tyrosine kinase potentiates NMDA receptor currents by reducing tonic zinc inhibition. Nat. Neurosci. *1*, 185–191.

Zimmer, J. and Haug, F.M. (1978). Laminar differentiation of the hippocampus, fascia dentata and subiculum in developing rats, observed with the Timm sulphide silver method. J. Comp. Neurol. *179*, 581–618.